Rare Metal Materials and Engineering
Volume 47, Issue 5, May 2018
Online English edition of the Chinese language journal

Available online at www.sciencedirect.com
ScienceDirect

Cite this article as: Rare Metal Materials and Engineering, 2018, 47(5): 1325-1332.

ARTICLE

Structure, Elastic Properties, Thermodynamic and Electronic Properties of Al-Y Alloy Under Pressure from First-principles Calculations

Niu Xiaofeng[1,3], Huang Zhiwei[2], Wang Han[1,3], Hu Lei[1,3], Wang Baojian[1,3]

[1] College of Materials Science and Engineering, Taiyuan University of Technology, Taiyuan 030024, China; [2] Southwest Technique and Engineering Institute, Chongqing 400039, China; [3] Shanxi Key Laboratory of Advanced Magnesium-Based Materials, Taiyuan 030024, China

Abstract: The influence of pressure on structure, elastic properties, thermodynamics and electronic properties of Al-Y alloy were investigated using first-principles. The equilibrium lattice constant, elastic constants, and elastic modulus as calculated here agree with results of previous studies. Calculated results of bulk modulus B, shear modulus G, Young's modulus E, Poisson's ratio v and Debye temperature Θ_D all increase as pressure increases, but the opposite is true for heat capacity c_p. In addition, the Debye temperature for the phases declines gradually as follows: Al_2Y>Al_3Y>AlY. Additionally, the G/B ratio indicates that AlY and Al_3Y are ductile materials, while Al_2Y is a brittle material, and that the ductility of AlY and Al_3Y can be improved with increased pressure, while the brittleness of Al_2Y does not improve with increased pressure. Finally, the paper presents and discusses calculations of density of states and charge populations as they are affected by pressure.

Key words: intermetallics; miscellaneous; elastic properties; thermodynamic and thermochemical properties; ab-initio calculations

Favorable physical characteristics make aluminum alloys a common material in the automotive and aerospace industries. These desirable properties include exceptional strength, light weight and welding performance [1-3]. At the same time, the usefulness of these alloys is limited by their poor performance at high temperatures [4]. Consequently, much work has been done to try to improve functionality of aluminum alloys. For a long time, rare earth element Y was to improve the tensile strength, resistance to heat and corrosion resistance and other characteristics of aluminum alloys [1].

The main purpose of using rare earth element Y in the aluminum alloys is the creation of AlY, Al_2Y and Al_3Y phases [5]. Recent experimental and theoretical studies have examined the AlY, Al_2Y and Al_3Y phases regarding their structure, mechanical properties and thermodynamics. For example, Timofeev et al.[5] conducted an experimental study of the effect of adding the Y element on the microstructures and mechanical properties of the AlY, Al_2Y and Al_3Y phases. Wang et al.[6] used the CALPHAD method to calculate lattice parameters, enthalpies of formation and mechanical properties for the Al-Y alloy. Huang et al. [7] applied first principles calculations to understand the electronic structure, elastic properties and thermodynamics of Al_2Y phases. Ciftciyo et al. [8] similarly used first principles calculations to study the structure, elastic and thermodynamic properties of Al_2Y under pressure. Duan et al. [9] explored the elastic properties of Al_3Y under high pressure using the Ab-initio method. Still, there are currently no reports on the impact of pressure on the structure and the thermodynamic and electronic properties of AlY, Al_2Y and Al_3Y. Pressure is an important factor in how the physical properties of a material behave, so an investigation of how external pressure influences the structure, elasticity and thermodynamics and electronic properties of Al-Y alloys will offer valuable insight into solid state theories and help establish the value of the basic parameters [10].

This paper examined multiple properties of AlY, Al_2Y and Al_3Y phase under pressure in the range of 0~50 GPa with a

Received date: May 14, 2017
Foundation item: National Natural Science Foundation of China (51574176); Program for the Top Young Academic Leaders of Higher Learning Institutions of Shanxi (TYAL) (143020142-S); Major Research & Development Plan of Shanxi Province (International Cooperation Project) (201603D421028)
Corresponding author: Niu Xiaofeng, Ph. D., Associate Professor, Taiyuan University of Technology, Taiyuan 030024, P. R. China, E-mail: niu.xiao.feng@126.com

step of 10 GPa. Those results were calculated using first principles calculations[11-13]. The properties of the AlY alloy phases were evaluated based on the following: the pressure dependence of the bulk modulus B, shear modulus G, Young's modulus E, Poisson's ratio v, Debye temperature Θ_D and heat capacity c_p. The results provide a valuable assessment of some properties which are difficult to measure by experimental methods.

1 Computational Methods

Calculations relating to the structure, elastic, thermodynamic and electronic properties of AlY, Al_2Y and Al_3Y phases used the Cambridge sequential total energy package (CASTEP) according to density functional theory (DFT)[14]. To determine the electronic exchange-correlation potential energy, the study used the generalized gradient approximation (GGA)[15] of the Perdew-Wang (PW91) [16] version. The plane wave cut off for kinetic energy was set to 300 eV[17]. In the Brillouin zone, the k point separation of the reciprocal space is 0.02 nm^{-1}, AlY is 8×8×8, Al_2Y is 4×4×4 and Al_3Y is 6×6×6. A finite basis set correction and the Pulay schemes[18] of density mixing were applied for the evaluation of energy and stress. Furthermore, our model used the BFGS scheme [19] to relax all atomic positions according to total energy and force according to the cell optimization criterion (RMs force of 5.0×10^{-5} eV/nm, stress of 0.01 GPa, and displacement of 5.0×10^{-5} nm). After the total energy and electronic structure were calculated, cell optimization follows, with SCF tolerance of 5.0×10^{-7} eV. The basis set for calculations was the states of Al 3s2 3p1 and Y 4d1 5s2.

2 Results and Discussion

2.1 Structural properties

Fig. 1 shows the crystal structure of AlY, Al_2Y and Al_3Y. Table 1 lists results of calculation for lattice parameters a_0, volume V_0, formation enthalpies ΔH, bulk modulus B_0 and pressure derivative B_0' at 0 GPa, together with other experimental[20,21] and theoretical data[6,7,22] that is available. As shown, the lattice parameter calculated here agrees with the other available data, and the formation enthalpies and bulk modulus are very close to previously reported results. The agreement between theoretical and experimental results indicates the high reliability of the present calculations.

The GGA method was used to calculate geometric optimization of cell volumes at different pressures in order to obtain bulk modulus B_0 and pressure derivative B_0'. The pressure-volumes obtained by this method were fitted to the third order Birch-Murnagham equation as follows [23],

$$P=\frac{3}{2}B_0[(\frac{V}{V_0})^{-7/3}-(\frac{V}{V_0})^{-5/3}]\cdot(1+\frac{3}{4}(B'-4)\cdot[(\frac{V}{V_0})^{-2/3}-1)] \quad (1)$$

The plots for the pressure-volume V/V_0 curves of AlY, Al_2Y and Al_3Y are shown in Fig.2. While the reduction of cell volume V/V_0 with the increasing pressure for each curve is easily observable, there is no experimental data available for comparison. According to the fitting of the pressure and cell volume V/V_0 curve, the following functions for AlY, Al_2Y and Al_3Y can be obtained:

$$V/V_0 = 0.9498 - 0.00765P + 5.3\times10^{-5}P^2 \quad (2)$$

$$V/V_0 = 0.9638 - 0.00708P + 4.75\times10^{-5}P^2 \quad (3)$$

$$V/V_0 = 0.9638 - 0.00736P + 5.2\times10^{-5}P^2 \quad (4)$$

2.2 Elastic properties

One important parameter of materials is the elastic constant, which often provides significant details about a material's mechanical stability [24]. Researching elastic constants at varying pressures is vital to understanding the mechanical properties of Al-Y alloys. The elastic constant of single crystals can be determined through geometric optimization.

The calculated Al-Y alloy phases in this paper are cubic crystals, for which the elastic constants are C_{11}, C_{12} and C_{44}. The following are the associated conditions of mechanical stability [26]: $C_{44}>0$, $C_{11}>|C_{12}|$, $C_{11}+2C_{12}>0$. Table 2 lists the calculated results for the elastic constants for three phases at zero pressure, along with experimental[20, 25] and theoretical values[6,7,9]. The data demonstrate that AlY, Al_2Y and Al_3Y easily fit the conditions for mechanical stability, and that there is good correspondence between the results of elastic constant calculations and the available theoretical and experimental data. Thus, the calculated elastic constants and conditions as selected should be appropriate. Fig.3a, which shows changes in the elastic constants under pressure, indicates that C_{11}, C_{12} and C_{44} increase as the pressure increases, and that C_{11} is more likely to change under pressure

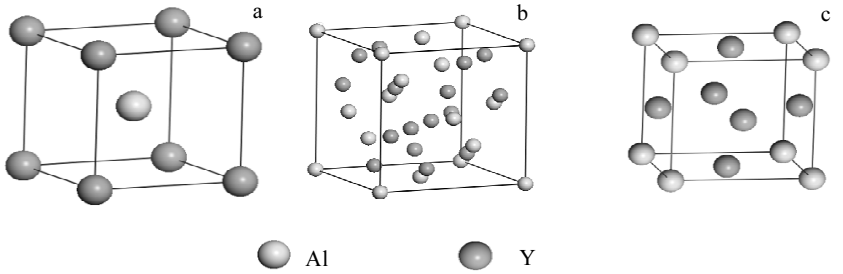

Fig. 1 Crystal structure of Al-Y alloy: (a) AlY, (b) Al_2Y, and (c) Al_3Y

Table 1 Calculated equilibrium lattice constant a_0, volume V_0, formation enthalpy, ΔH bulk modulus B_0 (GPa) and its first pressure derivative B_0' from the Birch-Murnaghan EOS of Al-Y alloy

Phase	Species	a_0/nm	$V_0/\times10^{-3}$ nm^3	ΔH/kJ·mol^{-1}	B_0/GPa	B_0'
AlY	Present	0.3625	47.646	−41.387	70.235	4.582
	Exp.[20]	0.3754	52.903	−54.91		
	Cal.[6]	0.3606	46.936	−40.16	63.47	3.95
Al_2Y	Present	0.7912	495.275	−52.972	80.764	4.175
	Exp.[20]	0.7861	485.773	−50.40	82.00	
	Cal.[6]	0.7880	489.504	−51.46	79.7	4.08
	Cal.[7]	0.772	460.099	−52.32	79.05	
Al_3Y	Present	0.4279	78.358	−42.471	77.901	4.143
	Exp.[21]	0.42326	75.827	−41.7	75.02	
	Cal.[22]	0.42597	77.292	−43.2	75.99	3.98
	Cal.[6]			−42.29	70.2	4.475

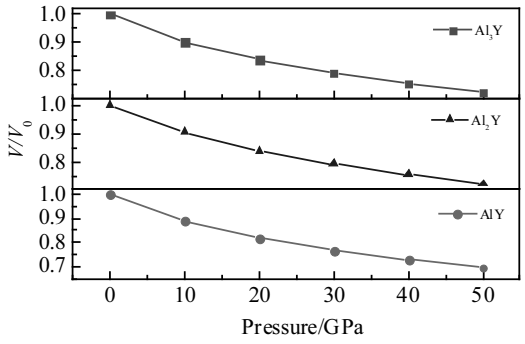

Fig.2 Variations of cell volume V/V_0 of AlY, Al_2Y and Al_3Y with pressure range from 0 to 50 GPa at 0 K

than C_{12} and C_{44} because C_{11} experiences length elasticity, while C_{12} and C_{44} experience shape elasticity, which makes them susceptible to a change in shape due to transverse strain, but not to a change in volume [8]. Therefore, C_{12} and C_{44} are less impressible compared with C_{11}.

The Voigte-Reusse-Hill method (VRH) was used to calculate the bulk moduli B, shear moduli G, Young's moduli E, and Poisson's ratio v of AlY, Al_2Y and Al_3Y [27]. For a cubic system, the calculation formulas are as follows [28]:

$$B = \frac{1}{3}(C_{11} + 2C_{12}) \tag{5}$$

$$G_V = \frac{1}{5}(3C_{44} + C_{11} - C_{12}) \tag{6}$$

$$G_R = \frac{5(C_{11} - C_{12})C_{44}}{3(C_{11} - C_{12}) + 4C_{44}} \tag{7}$$

$$G = \frac{1}{2}(G_V + G_R) \tag{8}$$

$$E = \frac{9GB}{3B + G} \tag{9}$$

$$\nu = \frac{(E - 2G)}{2G} \tag{10}$$

The calculated results of varying pressures for polycrystalline bulk modulus B, shear modulus G and Young's modulus E are shown in Fig.3b. Shear modulus G and bulk modulus B are accepted as measures of a material's resistance to changes in shape and volume, respectively[29]. As shown in Fig.3b, the bulk modulus calculations are much larger than those for shear modulus, which means that Al-Y phases resist changes in volume much better than they resist changes in shape. Young's modulus E is defined as the ratio between stress and strain,

Table 2 Calculated elastic constants C_{ij}, modulus ratio G/B, and Poisson's ratio v for AlY, Al_2Y and Al_3Y at 0 GPa

Phase		C_{11}/GPa	C_{12}/GPa	C_{44}/GPa	B/GPa	G/GPa	E/GPa	G/B	v
AlY	Present	93.765	58.469	65.028	70.235	38.716	98.119	0.552	0.267
	Exp.[25]	77.93	56.58	61.91	63.7				
	Cal.[6]	81.8	54.35	64.7	63.5	35.2	89.07	0.552	
Al_2Y	Present	167.781	37.256	57.476	80.764	60.474	145.185	0.748	0.201
	Exp.[20]	90.00	34.00	62.00	82.00	69.00	163.0	0.841	
	Cal.[6]	172.7	33.8	56.3	80.0	61.2	146.4	0.763	
	Cal.[7]	171.66	32.74	54.08	79.05	60.23	144.09	0.762	0.196
Al_3Y	Present	162.637	35.532	32.118	77.901	42.266	107.378	0.543	0.271
	Cal.[9]	163.44	35.77	32.28	78.66	42.8	107.1	0.598	

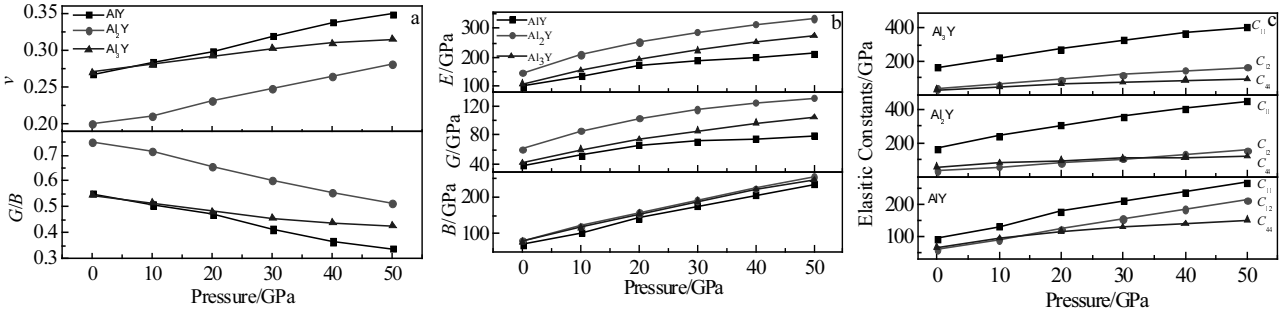

Fig.3 Elastic constants of AlY, Al_2Y and Al_3Y at different pressure: (a) *G/B*, Poisson's ratio *v*, (b) bulk modulus *B*-shear modulus *G*-Young's modulus *E*, and (c) elastic constants

and it can measure the stiffness of a solid. A larger value of *E* indicates better stiffness of a material [7]. The results shown in Fig.3b indicate the greatest stiffness in Al_2Y, followed by Al_3Y and finally AlY. The calculations indicate that *B, G* and *E* increase as external pressure grows, indicating that increasing pressure can improve hardness.

The ratios of *G/B* and Poisson's ratio *v* are shown in Fig.3c. Pugh[29] suggested predicting the brittleness of ductility of materials using the ratio of shear modulus to bulk modulus (*G/B*) of polycrystalline phases. Brittleness is indicated by a high *G/B* value, while ductility is associated with a low value. Ductility and brittleness separate at a value of about 0.57. The *G/B* values of AlY and Al_3Y phases are lower than 0.57, indicating they reveal ductility, while the *G/B* value of Al_2Y is larger than 0.57, indicating that Al_2Y is a brittle material. The calculated *G/B* values of AlY and Al_3Y decrease with increasing pressure, illustrating that increased pressure can improve ductility. On the contrary, the brittleness of Al_2Y deteriorates as pressure increases. The Poisson's ratio *v* quantifies the crystal's stability against shear[23], which usually ranges from 0.25 to 0.5. The calculated values of AlY, Al_2Y and Al_3Y phases at different pressure are in the range of 0.20~0.35 and increase as pressure increases, which indicates the centrality of interatomic forces.

2.3 Thermodynamic properties

A compound's elastic constants and its electronic structures can be determined by measuring the Debye temperature (Θ_D) and the compound's heat capacity at low temperature. The Debye temperature provides insights based on the elastic material's thermodynamic properties[7] because the measurement distinguishes between low and high temperature areas. For $T>\Theta_D$, the material has an energy of k_BT; and for $T<\Theta_D$ one predicts frozen state for high frequency materials[30]. The Θ_D can be calculated from the average sound velocity as follows [31, 32]:

$$\Theta_D = \frac{h}{k_B}\left[\frac{3n}{4\pi}\left(\frac{N_A\rho}{M}\right)\right]^{1/3} v_m \quad (11)$$

$$v_m = \left[\frac{1}{3}\left(\frac{2}{v_s^3} + \frac{1}{v_l^3}\right)\right]^{-1/3} \quad (12)$$

$$v_l = \sqrt{\left(B + \frac{4}{3}G\right)\frac{1}{\rho}} \quad (13)$$

$$v_s = \sqrt{G/\rho} \quad (14)$$

Where, k_B and *h* is the Boltzmann and Planck constant, respectively; N_A is the Avogadro number; *n* is the number of atoms per molecular formula; ρ is the density; *M* is the molecular mass; v_m, v_l and v_s are the average sound velocity, longitudinal sound velocity and the shear sound velocity, respectively.

The dependence of v_m, v_l and v_s with pressure ranging from 0 to 50 GPa are listed in Table 3. The calculated results of Θ_D at different pressures are shown in Fig.4. The Debye temperature of Al_2Y at 0 K and 0 GPa is 475.84 K, which is consistent with the available values 471.58 K [7] and 461.0 K[30] obtained from measuring elastic constants at room temperature. These results are close to our own, indicating that the previous result was calculated precisely and that the present results, as calculated, are accurate. The Θ_D of Al_2Y is the highest of the three phases. We also found that the Debye temperature increases as pressure increases for Al-Y phases, although the rate of increase gradually decreases. However, since it is difficult to compare our results regarding the Debye temperature of Al-Y phases at different pressures with calculated and experimental data, the calculated results presented here could be taken as a prediction for future research.

At the Fermi level, AlY, Al_2Y and Al_3Y have metallic features, so we can estimate the heat capacity (c_p) at the low-temperature based on calculations for the electronic structures and elastic constants[33]. These calculations are given as:

$$c_p(T) = \gamma T + \beta T^3 \quad (15)$$

$$\gamma = \frac{1}{3}\pi^2 k_B^2 D_f \quad (16)$$

$$\beta = \frac{12\pi^4 Rn}{5\Theta_D^3} \quad (17)$$

Table 3 Pressure dependence of shear (v_s) and longitudinal sound velocities (v_l), and average wave velocity (v_m) for AlY, Al_2Y and Al_3Y

Pressure/ GPa	AlY			Al_2Y			Al_3Y		
	v_m/m·s^{-1}	v_l/m·s^{-1}	v_s/m·s^{-1}	v_m/m·s^{-1}	v_l/m·s^{-1}	v_s/m·s^{-1}	v_m/m·s^{-1}	v_l/m·s^{-1}	v_s/m·s^{-1}
0	3444.25	5492.77	3096.08	4385.79	6489.77	3972.53	3817.83	6110.35	3430.80
10	3786.83	6174.74	3397.51	4982.61	7450.96	4507.76	4314.91	7012.99	3872.35
20	4101.38	6838.32	3673.14	5261.38	8031.70	4749.47	4628.79	7655.91	4148.09
30	4132.23	7160.02	3690.40	5423.23	8448.15	4885.68	4853.70	8154.83	4344.36
40	4118.83	7402.57	3669.76	5510.17	8762.95	4954.41	5025.97	8550.40	4494.39
50	4149.04	7647.99	3691.20	5553.87	9022.59	4984.42	5119.71	8787.53	4575.31

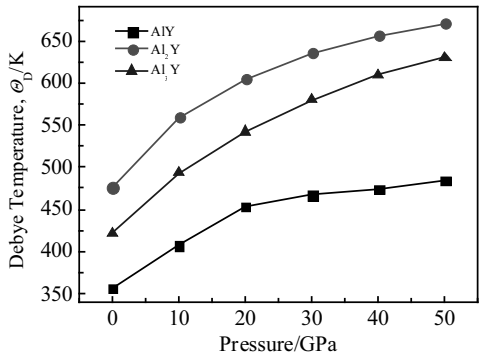

Fig.4 Debye temperature (Θ_D) of AlY, Al_2Y and Al_3Y at different pressure

Where γ is the coefficient of electronic structure; β represents lattice heat capacity; n and R are the total number of atoms per formula and molar gas constant, respectively. Another important tool for researching basic material properties is c_p. Note that Θ_D, in general, describes only the temperature dependence of c_p for $T<\Theta_D/10$ [34]. Thus, Fig.5 shows c_p versus T in the temperature range of the 0~35 K for three phases.

Fig. 5a~5c, show that the heat capacity for Al-Y phases increases as the temperature increases. The heat capacity differs at different pressure, which makes it clear that the heat capacity decreases as the pressure increases. As the

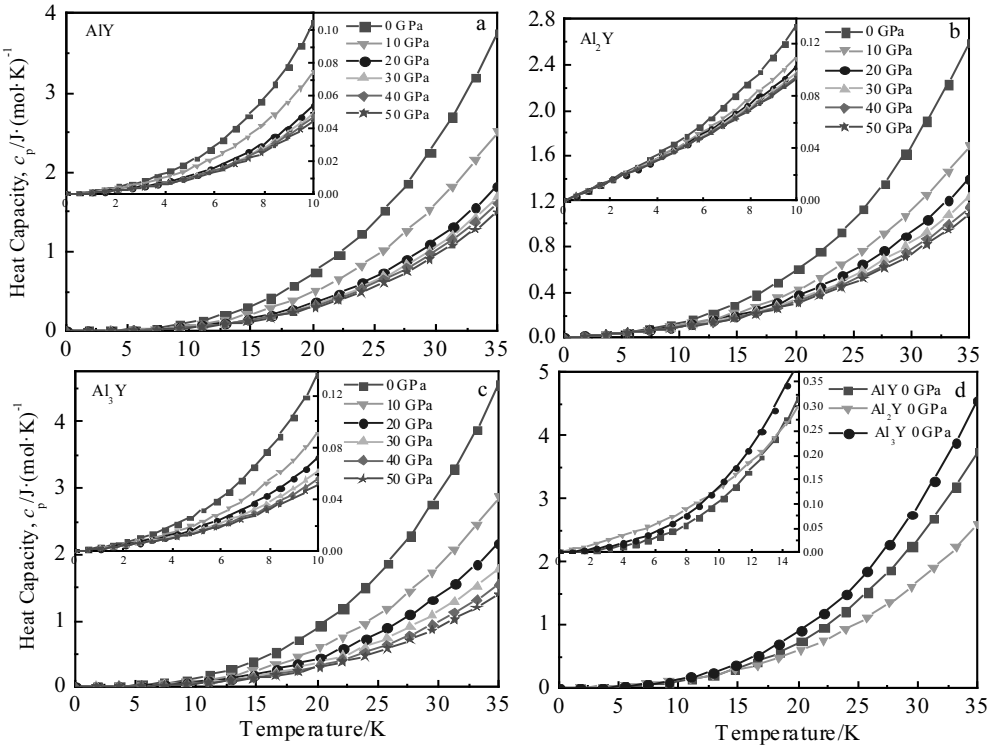

Fig.5 Temperature dependence of the heat capacity at different pressure for of AlY (a), Al_2Y (b), Al_3Y (c), and AlY-Al_2Y-Al_3Y at 0 GPa (d)

Table 4 Pressure dependence of the characteristic parameters of electron (γ) and phonon (β) specific heat for AlY, Al_2Y and Al_3Y

Pressure/ GPa	AlY		Al_2Y		Al_3Y	
	γ/ $\times10^{-3}$J $(K^2\cdot mol)^{-1}$	$\beta/\times10^{-5}$ $(K^4\cdot mol)^{-1}$	$\gamma/\times10^{-3}$ $J\cdot(K^2\cdot mol)^{-1}$	$\beta/\times10^{-5}$ $(K^4\cdot mol)^{-1}$	$\gamma/\times10^{-3}$ $J\cdot(K^2\cdot mol)^{-1}$	$\beta/\times10^{-5}$ $(K^4\cdot mol)^{-1}$
0	1.827184	8.595810923	7.822755	5.409413375	3.227909	10.37864921
10	1.666855	5.754219815	7.564908	3.336907768	2.653486	6.481763227
20	1.220246	4.164807806	7.528453	2.634627412	2.402362	4.876827489
30	1.128626	3.822822948	7.485369	2.271053423	2.232218	3.989186327
40	1.103073	3.661629752	7.418288	2.062832872	2.156973	3.423762268
50	1.067774	3.422264575	7.403139	1.931910238	2.107754	3.102900255

temperature increases to 9.5 K, electron excitation is the main contributor to c_p (Fig.5d). The values of c_p have the following growth trend: Al_2Y>Al_3Y>AlY, which is close to the trend of γ (Table 4), indicating that heat capacities are determined first by electrons. In the temperature range of 9.5~13.5 K, the growth sequence of c_p is Al_3Y> Al_2Y > AlY, indicating that excitation of both electrons and phonons contributes to c_p. Finally, in the temperature range of 13.5~35 K, phonon excitation is the main contributor to c_p, resulting in a growth trend of Al_3Y>AlY>Al_2Y. Therefore, it can be observed that as temperature increases, heat capacities of AlY alloys are first determined by electron excitation, then by excitation of electrons and phonon, and finally by phonon excitation.

2.4 Electronic properties

To further understand the bonding features of Al-Y alloys and how pressure influences their electronic structure, it is necessary to calculate the alloy's local density of states (PDOS) and total density of states (TDOS). The PDOS of Al-Y alloy is illustrated in Fig.6, and TDOS only under pressures of 0, 30 and 50 GPa are shown in Fig.7.

In Fig.6, we see that many energy states cross the Fermi level, which indicates that AlY, Al_2Y and Al_3Y phases demonstrate metallic properties. Furthermore, the peaks of bonding for all phases can be found in a range of —10 to 15 eV, and those peaks arise from valence electron number contributions of the Al(s), Al(p), Y(s) and Y(p) orbits for AlY, Al_2Y and Al_3Y (Fig.6a~6c). Moreover, it is obvious that hybridization between Al and Y atoms forms a covalent

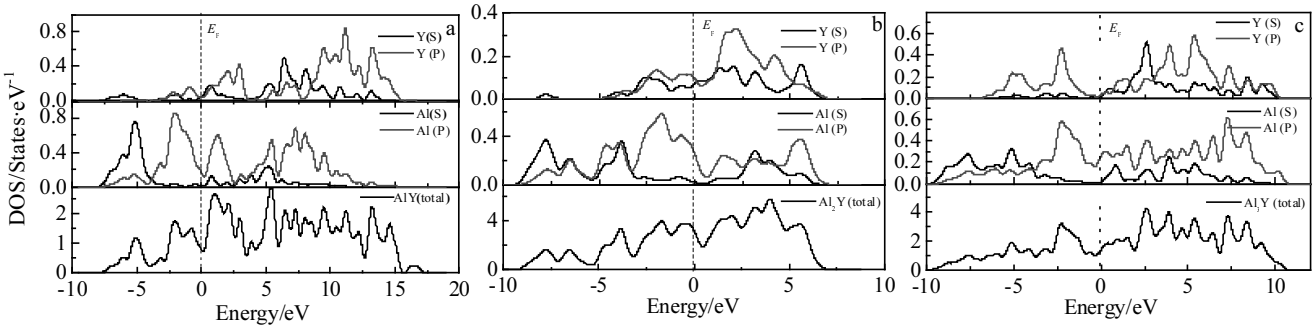

Fig.6 Total and partial density of states at 0 GPa: (a) AlY, (b) Al_2Y, and (c) Al_3Y

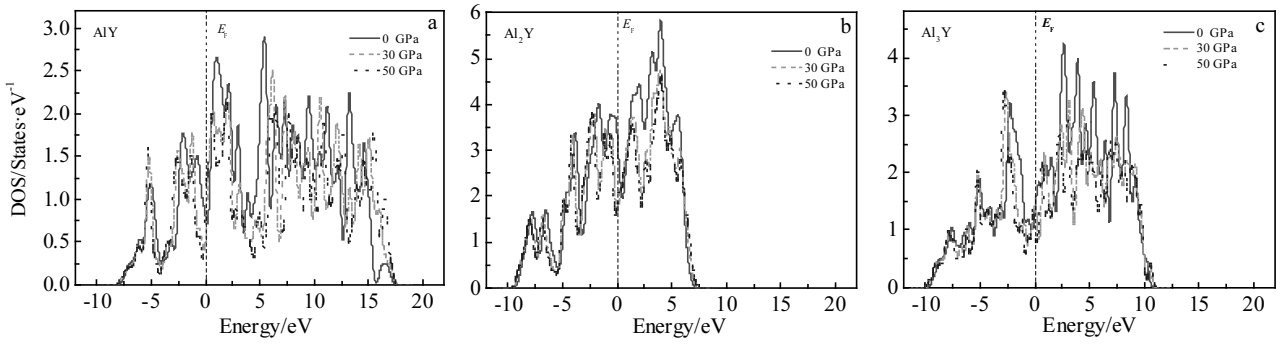

Fig. 7 Total density of states of AlY (a), Al_2Y (b), and Al_3Y (c) at different pressure

Table 5 Mulliken charges of AlY, Al_2Y and Al_3Yphasesat different pressure

Pressure/ GPa	AlY	Al_2Y	Al_3Y
	Mulliken charge (e)	Mulliken charge (e)	Mulliken charge (e)
0	$Al^{-0.43}$ $Y^{+0.43}$	$Al^{-0.37}$ $Y^{+0.75}$	$Al^{-0.09}Y^{+0.28}$
30	$Al^{-0.22}$ $Y^{+0.22}$	$Al^{-0.41}$ $Y^{+0.82}$	$Al^{-0.70}$ $Y^{+2.09}$
50	$Al^{-0.07}$ $Y^{+0.07}$	$Al^{-0.43}$ $Y^{+0.86}$	$Al^{-0.98}$ $Y^{+2.95}$

bonding feature. Fig.6d shows that the bonding electron numbers per atom of Al_3Y are 2.997 between the Fermi level and —10 eV, whereas for each atom of Al_2Y the number is greater (5.994), and for each atom of AlY the number is smaller (2.992). Since a smaller bonding electron number indicates a weaker charge interaction[34], the results indicate that Al_2Y has the greatest structural stability, followed by Al_3Y and finally AlY.

TDOS of Al-Y phases at pressure of 0, 30 and 50 GPa are shown in Fig. 7. As can be seen, the change in TDOS curve shapes is slight, indicating that the AlY, Al_2Y and Al_3Y phases maintain structural stability and experience no structural changes under pressure up to 50 GPa. Since TDOS decreases as external pressure increases, it can be deduced that variations of interaction potentials happen in AlY, Al_2Y and Al_3Y phases because interatomic distances shrink under pressure, thus reducing total electronic energy levels.

2.5 Charge populations

Charge populations and valence orbit track occupancies were calculated to gain further insight to the relative covalence and ionicity of AlY, Al_2Y and Al_3Y phases under different pressures; the results are shown in Table 5. The (+) and (—) represent gains and losses of electronic charge, respectively. The calculated values demonstrate that for Al_2Y and Al_3Y phases, charge transfer from Al atoms to Y atoms increases as pressure increases, but for AlY phases charges transfer decreases as pressure increases. These observations can be regarded as predictive for future experiments. It is also worth noting that while the basis set largely determines the absolute magnitudes of the atomic charges in the population analysis [35], the observed trend in charge transfers is significant for a better understanding of bonding characteristics.

3 Conclusions

1) The calculated equilibrium lattice constants, elastic constants, and elastic modulus are consistent with existing experimental and theoretical outcomes. The pressure derivative B_0' for AlY, Al_2Y and Al_3Y phases are 4.582, 4.175, and 4.143 GPa, respectively.

2) The Al-Y phases retain mechanical stability as pressure increases from 0 to 50 GPa. Whereas the calculated results of bulk modulus B, shear modulus G, Young's modulus E and Poisson's ratio v increase as pressure increases, while the impact of pressure on heat capacity c_p is opposite. The ratio of G/B shows that AlY and Al_3Y are ductile materials, while Al_2Y is brittle material, and that the ductility of AlY and Al_3Y can be improved by increasing pressure, but the brittleness of Al_2Y cannot be improved with increased pressure.

3) The Debye temperature as calculated for all Al-Y phases at 0 K are consistent with experimental results. The Debye temperature of Al-Y alloys increases as pressure increases, with Al_2Y having the highest Debye temperature.

4) The bonding electron numbers show that the structural stability of these phases decreases in the following sequence: Al_2Y> Al_3Y>AlY. Additionally, the Al-Y phases experience no structural changes when pressure is up to 50 GPa. Finally, charge population analysis demonstrates that charge transfer in Al_2Y and Al_3Y phases from Al atoms to Y atoms increases while pressure increases, but charge transfer in AlY phases decreases as pressure increases.

References

1 Rosalbino F, Angelini E, Negri S D *et al*. *Intermetallics*[J], 2003, 11(5): 435

2 Norman A F, Hyde K, Costello F *et al*. *Materials Science & Engineering A*[J], 2003, 354(S1-2): 188

3 Jun J H, Kim J M,Seong K D *et al*. *Materials Science Forum*[J], 2005, 475-479: 441

4 Senkov O N, Shagiev M R, Senkova S V *et al*. *Acta Materialia*[J], 2008, 56(15): 3723

5 Timofeev V S, Turchanin A A, Zubkov A A *et al*. *Thermochimica Acta*[J], 1997, 299: 37

6 Wang Jiong, Shang Shunli, Wang Yi *et al*. *Fuel & Energy Abstracts*[J], 2011, 35(4): 151

7 Huang Z W, Zhao Y H, Hou H *et al*. *Physica B Condensed Matter*[J], 2012, 407(7): 1075

8 Ciftci Y O, Colakoglu K, Delizobz E *et al*. *Journal of Materials Science & Technology*[J], 2012, 28(2): 155

9 Duan Y H, Sun Y, Peng M J *et al*. *Journal of Alloys & Compounds*[J], 2014, 590(5): 50

10 Bouhemadou A, Khenata R. *Journal of Applied Physics*[J], 2007, 102(4): 043 528

11 Duan Yonghua. *Rare Metal Materials and Engineering*[J], 2015, 44(1): 18

12 Hu Jieqiong, Xie Ming, Zhang Jiming, *et al*. *Rare Metal Materials and Engineering*[J], 2015, 44(11): 2677

13 Liu Zheng, Ju Yang, Mao Pingli *et al*. *Rare Metal Materials and Engineering*[J], 2015, 44(11): 2775

14 Shi Dongmin, Wen Bin, Melnik R *et al*. *Journal of Solid State Chemistry*[J], 2009, 182(10): 2664

15 Pack J D, Monkhors H J. *Phys Rev B* [J], 1977, 16: 1748

16 Perdew J P, Burke K, Ernzerhof M. *Phys Rev Lett*[J], 1996(7): 1396
17 Nylen J, Garcia F J, Mosel B D *et al*. *Cheminform*[J], 2004, 6(1):147
18 Hamme R B, Hansen L B, Norskov J K. *Physical Review B*[J], 1999, 59(11): 7413
19 Fischer T H. *Journal of Physical Chemistry*[J], 1992, 96(24): 9768
20 Villars P, Calvert L D. Pearson's Hanbook of Crystallographic Date for intermetallic Phases[M]. Ohio: ASM International, Materials Park, 1991
21 Tao Xiaoma, Ouyang Yifang, Liu Huashan *et al*. *International Journal of Materials*[J], 2008, 99(6): 582
22 Zhang Xudong, Wang Shaoqing. *Compute Mater Sci*[J], 2014, 90: 56
23 Birch F. *J Geophys Res; (United States)*[J], 1978, 83(B3): 1257
24 Wang Jingyang, Zhou Yanchun. *Phys Rev*[J], 2004, 69(21): 1681
25 Wang H Y, Gao X Y, Zeng J M *et al*. *Rare Metal Materials and Engineering*[J], 2017, 46(3): 735 (in Chinese)
26 Tao Xiaoma, Ouyang Yifang, Liu Huashan *et al*. *Physica B Condensed Matter*[J], 2007, 399(1): 27
27 Hill R. *Proceedings of the Physical Society A*[J], 1952, 65(5): 349
28 Wu Zhijian, Zhao Erjun, Xiang Hongping *et al*. *Physical Review B*[J], 2007, 76(5): 4115
29 Pughs F X. *London Edinburgh & Dublin Philosophical Magazine & Journal of Science*[J], 1954, 45(367): 823
30 Mayer B, Anton H, Bott E *et al*. *Intermetallics*[J], 2003, 11(1): 23
31 Deligoze, Ciftcib Y O, Jochymc P T *et al*. *Materials Chemistry & Physics*[J], 2008, 111: 29
32 Sinko G V, Smirnowna. *Journal of Physics Condensed Matter*[J], 2002, 14(29): 6989
33 Chen Qiang, Huang Zhiwei, Zhao Zude *et al*. *Computational Materials Science*[J], 2013, 67: 196
34 Zhou D W, Liu J S, Xu S H *et al*. *International Conference of Molecular Simulations & Applied Informatics Technologies*[J], 2010, 405(13): 2863
35 Li Zuo, Wang Pu, Chen Haihua *et al*. *Physica B Condensed Matter*[J], 2011, 406(5): 1182

第一性原理研究 Al-Y 合金在压力作用下的晶胞结构、力学性质、热力学性质和电子结构

牛晓峰[1,3]，黄志伟[2]，王 涵[1,3]，胡 磊[1,3]，王宝健[1,3]
(1. 太原理工大学 材料科学与工程学院，山西 太原 030024)
(2. 中国兵器工业第五九研究所，重庆 400039)
(3. 太原理工大学 先进镁基材料山西省重点实验室，山西 太原 030024)

摘 要：采用基于密度泛函理论的第一性原理研究了压力对 Al-Y 合金的晶胞结构、力学性质、热力学性质和电子结构的影响。结果表明：晶格常数、弹性常数和弹性模量的计算结果与先前理论计算和实验结果相一致；体模量、剪切模量、杨氏模量、泊松比和德拜温度随压力增大而增大，而热熔则随压力的增大而减小； 德拜温度按 $Al_2Y > Al_3Y > AlY$ 顺序逐步降低； 通过 Pugh 准则（GB）预测出 AlY 和 Al_3Y 相是塑性材料，并随压力的增大塑性增加，而 Al_2Y 相是脆性材料，其脆性并未随压力增大得到改善；最后还分析了压力对 AlY 、Al_2Y 和 Al_3Y 相的态密度和电荷布局的影响。

关键词：中间合金；力学性质；热力学性质；从头计算法

作者简介：牛晓峰， 男，1982 年生，博士，副教授，太原理工大学材料科学与工程学院，山西 太原 030024， E-mail: niu.xiao.feng@126.com